

# Edit2Restore: Few-Shot Image Restoration via Parameter-Efficient Adaptation of Pre-trained Editing Models

M. Akin Yilmaz<sup>1</sup>[0000-0002-0795-8970], Ahmet Bilican<sup>2</sup>[0009-0000-6406-8168],  
Burak Can Biner<sup>1</sup>[0009-0009-8580-8220], and  
A. Murat Tekalp<sup>2</sup>[0000-0003-1465-8121]

<sup>1</sup> Codeway AI, Istanbul, Turkey

<sup>2</sup> Koc University, Istanbul, Turkey

**Abstract.** Image restoration has traditionally required training specialized models on thousands of paired examples per degradation type. We challenge this paradigm by demonstrating that powerful pre-trained text-conditioned image editing models can be efficiently adapted for multiple restoration tasks through parameter-efficient fine-tuning with remarkably few examples. Our approach fine-tunes LoRA adapters on FLUX.1 Kontext, a state-of-the-art 12B parameter flow matching model for image-to-image translation, using only 16-128 paired images per task, guided by simple text prompts that specify the restoration operation. Unlike existing methods that train specialized restoration networks from scratch with thousands of samples, we leverage the rich visual priors already encoded in large-scale pre-trained editing models, dramatically reducing data requirements while maintaining high perceptual quality. A single unified LoRA adapter, conditioned on task-specific text prompts, effectively handles multiple degradations including denoising, deraining, and dehazing. Through comprehensive ablation studies, we analyze: (i) the impact of training set size on restoration quality, (ii) trade-offs between task-specific versus unified multi-task adapters, (iii) the role of text encoder fine-tuning, and (iv) zero-shot baseline performance. While our method prioritizes perceptual quality over pixel-perfect reconstruction metrics like PSNR/SSIM, our results demonstrate that pre-trained image editing models, when properly adapted, offer a compelling and data-efficient alternative to traditional image restoration approaches, opening new avenues for few-shot, prompt-guided image enhancement. The code to reproduce our results are available at: <https://github.com/makinyilmaz/Edit2Restore>

**Keywords:** few-shot image restoration · pre-trained image editing models · parameter-efficient adaptation.

## 1 Introduction

Image restoration, recovering high-quality images from degraded observations, has traditionally relied on training specialized models for each degradation type,

requiring thousands of paired training examples per task. Recent all-in-one restoration methods [12, 21, 33] attempt to handle multiple degradations within a unified framework, yet still demand extensive paired datasets and specialized architectures trained from scratch. For example, InstructIR [12] requires training a restoration network with over 10,000 synthetically generated text prompts and thousands of image pairs per degradation to achieve state-of-the-art results.

We pose a **fundamental question**: *Can powerful pre-trained image editing models be efficiently adapted for image restoration with dramatically fewer training examples?* Recent advances in image generation and editing have produced remarkable models like FLUX.1 Kontext [5] with sophisticated understanding of image structure, quality, and semantics learned from enormous datasets. These models excel at text-conditioned image-to-image translation tasks such as object removal, style transfer, and content modification. However, their potential for inverse problems, specifically image restoration, remains largely unexplored in the few-shot regime.

In this work, we demonstrate that FLUX.1 Kontext [5], a prominent text-conditioned image editing model based on rectified flow matching, can be efficiently adapted for multiple restoration tasks using remarkably few examples: just 16-128 paired images per task. FLUX.1 Kontext is a 12 billion parameter model designed for image-to-image translation, capable of performing diverse editing operations guided by natural language instructions. Our **key insight** is that *the visual understanding already encoded in such models including knowledge about image quality, degradation patterns, and natural statistics can be efficiently transferred to restoration tasks through parameter-efficient fine-tuning (PEFT), without requiring the model to be trained from scratch.*

We fine-tune lightweight LoRA [15] adapters on FLUX.1 Kontext, guided by simple text prompts that specify the restoration operation ('remove the noise from the image', 'remove the haze from the image', 'remove the rain from the image'). The model performs image-to-image translation: given a degraded input image and a restoration instruction, it generates the corresponding clean output. Unlike InstructIR which trains specialized restoration networks from scratch, we leverage the pre-trained visual understanding already embedded in large-scale image editing models. A single unified LoRA adapter, conditioned on task-specific text prompts, effectively handles multiple degradations including denoising, deraining, and dehazing, all learned from minimal training data.

Unlike traditional image restoration methods that are optimized for pixel-level reconstruction metrics (PSNR/SSIM) using  $\ell_1$  or  $\ell_2$  losses, our approach is based on optimization of perceptual image quality similar to flow matching-based editing models. While we report PSNR/SSIM for completeness, our primary focus is on perceptual visual quality. This reflects a fundamental trade-off: pixel-perfect reconstruction versus perceptually plausible restoration.

Overall, we can summarize our contributions as follows:

- We present the first approach demonstrating that pre-trained text-conditioned image editing models can be effectively adapted for image restoration with minimal paired data, achieving orders of magnitude better data efficiency than existing methods requiring thousands of examples.

- We introduce a parameter-efficient fine-tuning framework where a single LoRA adapter handles multiple restoration tasks (denoising, deraining, dehazing) through natural language instructions, eliminating the need for task-specific architectures.
- We conduct extensive ablations examining: the relationship between training set size and restoration quality, establishing performance bounds from 16 to 128 images; trade-offs between task-specific versus unified multi-task LoRA training; impact of fine-tuning text encoders versus keeping them frozen.
- We demonstrate that leveraging visual priors from pre-trained image editing models opens a compelling alternative pathway for image restoration, one that prioritizes perceptual quality and data efficiency over pixel-perfect metrics, enabling practical few-shot learning scenarios.

## 2 Related Work

### 2.1 Task-Specific Image Restoration Models

Image restoration aims to recover high-quality images from degraded observations. Early research developed specialized models for specific degradation types, including denoising [47], deblurring [19, 32], low-light enhancement [7, 42], dehazing [35], deraining [17], desnowing [10, 27], and raindrop removal [34]. CNN-based methods like NAFNet [8], MPRNet [46], and HINet [9], followed by transformer based approaches such as Restormer [45], SwinIR [23], and Uformer [41] advanced the field through better architectural designs. However, these methods optimize pixel-level metrics, using  $\ell_1$  or  $\ell_2$  losses, requiring thousands of paired data per task and fall short in naturalness (perceptual quality).

### 2.2 Multi-Task Image Restoration Models

Recent work has explored models capable of handling multiple restoration tasks. Among these, AirNet [21] employed contrastive learning to distinguish degradation types. Prompt-based methods [12, 22, 30, 33, 38] introduced learnable parameters or natural language instructions to encode degradation-specific information, guiding restoration backbones like NAFNet [8] and Restormer [45]. For instance, InstructIR [12] uses human-written text prompts to achieve strong results across multiple tasks. However, these methods train restoration networks from scratch, requiring thousands of paired images per task and substantial computational costs. Only recent work like LoRA-IR [1] has explored parameter-efficient adaptation through low-rank techniques.

With the success of diffusion models in generation, several works leverage diffusion priors for restoration [2, 18, 24, 29, 40, 48]. While effective, most diffusion-based approaches are computationally expensive and require large data.

Our work differs fundamentally from the state of the art: rather than training specialized architectures from scratch, we adapt pre-trained image editing models with remarkably few examples, demonstrating that powerful visual priors from large-scale generative training can be efficiently transferred to restoration through parameter-efficient fine-tuning.

### 2.3 Text-Conditioned Image Editing Models

Recent text-conditioned image editing models excel at modifying images according to natural language instructions while preserving unrelated content. Early work like InstructPix2Pix [6] demonstrated instruction-following editing, while recent models achieve state-of-the-art quality: FLUX.1 Kontext [5] employs a dual-stream architecture processing image and text separately, Qwen-Image-Edit [43] offers a competitive alternative, and unified models [11, 31, 44] handle both understanding and generation within single architectures.

These models benefit from pre-training on billions of image-text pairs, learning rich visual priors about image structure, quality patterns, and natural statistics. Modern architectures combine semantic features from vision-language models with reconstructive features from VAE encoders, achieving both semantic coherence and visual fidelity.

Our key insight is that image-to-image translation aligns naturally with image-to-image restoration: transforming degraded inputs to clean outputs via text instructions is fundamentally an editing operation. Rather than training from scratch, we demonstrate that parameter-efficient fine-tuning of these pre-trained priors requires only 16-128 examples per task, dramatically reducing data requirements while achieving competitive quality.

### 2.4 Parameter-Efficient Fine-Tuning

Parameter-efficient fine-tuning (PEFT) methods [4, 15, 49] enable adapting large pre-trained models to new tasks while training only a small fraction of parameters. LoRA (Low-Rank Adaptation) [15] injects trainable low-rank matrices into model layers, achieving strong performance in language and vision tasks with minimal parameters.

We demonstrate that LoRA adaptation of FLUX.1 Kontext, when combined with proper text conditioning and limited paired data, enables effective multi-task restoration. Our comprehensive ablations examine rank selection, text encoder training strategies, and the effectiveness of parameter-efficient adaptation for few-shot restoration, providing insights for future research in this direction.

## 3 Edit2Restore: Proposed Methodology

We propose a PEFT approach for adapting a pre-trained image editing model to text-conditioned multi-task image restoration with minimal training data. Our method leverages FLUX.1 Kontext [5], a 12 billion parameter flow matching model designed for text-conditioned image-to-image translation, and adapts it to multi-task image restoration through Low-Rank Adaptation (LoRA) [15]. Figure 1 illustrates our overall framework.

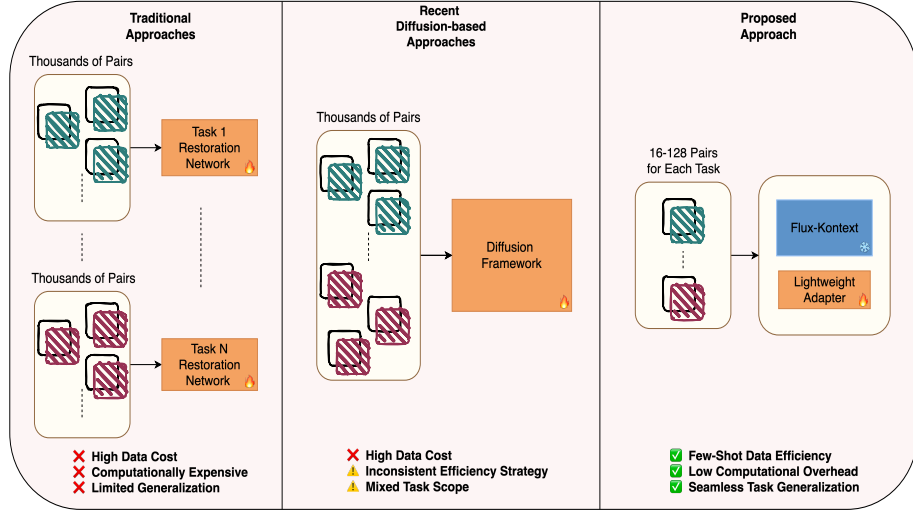


**Fig. 1.** Traditional approaches require training specific models with thousands of paired examples for each restoration task. Recent diffusion-based multi-task image restoration models leverage strong priors but still demand extensive paired data to train from scratch. Our approach achieves few-shot efficiency by adapting pre-trained image editing models with only 16-128 examples per task through parameter-efficient fine-tuning.

### 3.1 Preliminaries: FLUX.1 Kontext

FLUX.1 Kontext is a rectified flow transformer that performs image-to-image translation conditioned on both text instructions and input images. Given a degraded image  $\mathbf{x}_{\text{deg}} \in \mathbb{R}^{H \times W \times 3}$  and a text prompt  $\mathbf{t}$  describing the desired restoration operation, the model generates a restored image  $\mathbf{x}_{\text{res}}$  through an iterative flow matching process in latent space.

The model consists of three main components that work together to generate images. A variational autoencoder with 16 latent channels encodes images into latent representations  $\mathbf{z} = \mathcal{E}(\mathbf{x})$  and decodes them back to pixel space  $\mathbf{x} = \mathcal{D}(\mathbf{z})$ . Two text encoders, CLIP [36] and T5 [37], process the text prompt  $\mathbf{t}$  into embeddings that condition the generation process. Finally, a flow matching transformer with a hybrid architecture combining double-stream and single-stream transformer blocks operates on the latent space, performing iterative refinement guided by text conditioning.

Unlike traditional diffusion models that predict noise, FLUX.1 Kontext uses rectified flow matching [25,26] which learns to predict velocity fields. The forward process constructs a linear interpolation path between clean latent  $\mathbf{z}_{\text{clean}}$  and Gaussian noise  $\epsilon \sim \mathcal{N}(0, \mathbf{I})$ :

$$\mathbf{z}_t = (1 - t)\mathbf{z}_{\text{clean}} + t\epsilon \quad (1)$$

where  $t \in [0, 1]$  is the timestep. The model learns to predict the velocity  $\mathbf{v} = \epsilon - \mathbf{z}_{\text{clean}}$  that connects the two endpoints. This formulation provides straighter

generation trajectories compared to standard diffusion processes, enabling faster and more stable sampling.

FLUX.1 Kontext is pre-trained on billions of image-text pairs, learning rich priors about image structure, quality, and editing operations. Our key insight is that these pre-trained representations already encode knowledge about degradations and can be efficiently adapted for restoration.

### 3.2 LoRA for Image Restoration

Rather than fine-tuning all 12 billion parameters of FLUX.1 Kontext, we employ Low-Rank Adaptation to inject trainable parameters efficiently. For a pre-trained weight matrix  $\mathbf{W}_0 \in \mathbb{R}^{d \times k}$  in the transformer layers, LoRA constrains the weight update through low-rank decomposition:

$$\mathbf{W} = \mathbf{W}_0 + \Delta\mathbf{W} = \mathbf{W}_0 + \mathbf{B}\mathbf{A} \quad (2)$$

where  $\mathbf{B} \in \mathbb{R}^{d \times r}$  and  $\mathbf{A} \in \mathbb{R}^{r \times k}$  with rank  $r \ll \min(d, k)$ . During training,  $\mathbf{W}_0$  remains frozen while  $\mathbf{B}$  and  $\mathbf{A}$  are trained.

We apply LoRA to the attention projection layers in the flow matching transformer. Specifically, we inject LoRA adapters into the query, key, and value projection matrices of each attention block. This results in a small fraction of trainable parameters, while maintaining the model’s expressive capacity for the restoration task.

### 3.3 Text Prompt Design

We use simple, consistent prompts for each restoration task. Our prompt design follows the template:

"remove the [degradation] from the image"

where [degradation] is replaced with the specific corruption type ('noise', 'rain', 'haze'). This simplicity serves two purposes: (1) it leverages FLUX.1 Kontext’s pre-trained understanding of editing instructions without requiring extensive prompt engineering, and (2) it enables straightforward multi-task learning where the model learns to distinguish tasks primarily through the prompt conditioning.

For the unified multi-task setting, we condition each training sample on its corresponding task-specific prompt, allowing a single LoRA adapter to handle multiple degradation types. During inference, the appropriate prompt is provided to guide the restoration process.

## 4 Experiments

We present comprehensive experiments analyzing our parameter-efficient adaptation approach for image restoration. Our evaluation focuses on establishing performance bounds, investigating the impact of training set size, and examining key design choices including text encoder fine-tuning and multi-task versus single-task learning strategies.

#### 4.1 Experimental Setup

**Datasets.** We construct small training sets by sampling paired images from established restoration benchmarks. For denoising, we sample from BSD400 [3]; for deraining, from Rain100L [13]; and for dehazing, from the Reside (outdoor) SOTS [20] dataset. For denoising, we ensure balanced coverage across noise levels by generating approximately equal numbers of degraded images at  $\sigma = 15, 25, 50$ .

For evaluation, we use standard benchmarks: BSD68 for denoising (at noise levels  $\sigma = 15, 25, 50$ ), Rain100L for deraining, and 500 images from the SOTS outdoor set for dehazing. These datasets provide diverse test conditions to assess generalization beyond the limited training samples.

**Image resolution handling.** During training, all samples are resized to  $1024 \times 1024$  resolution. At test time, input images are first resized to  $1024 \times 1024$  for processing, and the restored output is then resized back to the original resolution, ensuring compatibility with arbitrary input dimensions while maintaining the model’s expected operating resolution.

**Implementation details.** All experiments are conducted on a single NVIDIA H100 GPU. The LoRA rank and batch size are set to 64, 4 respectively for all experiments. Each training run is performed for 1,920 iterations across all experimental configurations to ensure fair comparison. For multi-task training with three degradation types (denoising, deraining, dehazing), this corresponds to approximately 640 iterations per task when using 32 images per task (96 total images with batch size 4). We employ the AdamW optimizer [28] with learning rate  $1 \times 10^{-4}$  for the transformer LoRA parameters. When fine-tuning the text encoder, we use a lower learning rate of  $5 \times 10^{-6}$  to prevent catastrophic forgetting of pre-trained text representations. Weight decay is set to  $1 \times 10^{-4}$  for transformer parameters and  $1 \times 10^{-3}$  for text encoder parameters. We apply a constant learning rate schedule with 500 warmup steps. Training is performed in mixed precision (bfloating16) with gradient checkpointing enabled to reduce memory consumption.

During training, we use logit-normal timestep sampling with  $\mu = 0.0$  and  $\sigma = 1.0$  for the rectified flow matching objective. Dataset entries are shuffled before training to mix all degradation types uniformly across batches. During inference, we follow the rectified flow sampling procedure. Starting from pure noise, we iteratively integrate the learned velocity field to generate the clean latent. For all experiments, we use 28 integration steps and set the guidance scale to 2.5 following FLUX.1 Kontext’s default sampling schedule. Inference takes approximately 15-20 seconds per image at  $1024 \times 1024$  resolution on a single H100 GPU.

**Evaluation metrics.** We report three complementary metrics to assess restoration quality from different perspectives: (1) **FID (Fréchet Inception Distance)** [14] measures distribution-level similarity between restored and ground truth images, capturing overall perceptual quality and realism; (2) **CMMMD (CLIP Maximum Mean Discrepancy)** [16] evaluates feature-space similarity using maximum mean discrepancy, providing a robust measure of distribution matching; (3) **CLIP-IQA** [39] assesses perceptual image quality using CLIP-

**Table 1.** Effect of LoRA fine-tuning compared to zero-shot baseline. Both fine-tuned configurations use LoRA rank  $r = 64$  trained on 128 image pairs per task. TF and TE stand for Transformer and Text Encoder respectively. Metrics reported as FID/CMMD/CLIP-IQA (lower/lower/higher is better).

Configuration	Dehazing	Deraining	Denoising BSD68		
	SOTS	Rain100L	$\sigma = 15$	$\sigma = 25$	$\sigma = 50$
Baseline (No LoRA)	24.15/0.41/0.72	37.68/0.52/0.90	29.62/0.54/0.80	45.93/0.70/0.76	81.75/0.94/0.73
LoRA: TF	15.74/0.13/0.60	12.36/0.42/0.91	30.53/0.68/0.89	36.08/0.72/0.87	51.98/0.73/0.86
LoRA: TF + TE	15.05/0.12/0.59	11.76/0.40/0.91	28.80/0.56/0.89	36.60/0.65/0.88	52.13/0.67/0.88

based features, aligning with human perception of visual quality. These metrics prioritize perceptual quality over pixel-perfect reconstruction, consistent with our approach’s focus on leveraging pre-trained generative priors rather than optimizing for PSNR/SSIM.

## 4.2 Zero-Shot Baseline and Text Encoder Fine-tuning

To establish the effectiveness of our parameter-efficient adaptation approach, we first evaluate FLUX.1 Kontext’s zero-shot restoration capabilities without any fine-tuning. This baseline examines whether the model’s pre-trained understanding can perform text-guided degradation removal using only task-specific prompts like *remove the haze from the image*.

**Baseline Performance** Table 1 presents our findings comparing the baseline against LoRA-adapted configurations. The baseline results reveal significant limitations in the model’s inherent restoration capabilities. On dehazing, the baseline achieves FID/CMMD/CLIP-IQA of 24.15/0.41/0.72, while deraining produces 37.68/0.52/0.90. The denoising results are particularly telling: performance degrades substantially at higher noise levels, with FID increasing from 29.62 at  $\sigma = 15$  to 81.75 at  $\sigma = 50$ . These results confirm that while FLUX.1 Kontext possesses rich visual priors from editing pre-training, these priors alone are insufficient for effective restoration without task-specific adaptation.

**Parameter-efficient fine-tuning.** When the model transformer is fine-tuned using LoRA adapters, substantial improvements are observed across nearly all tasks. Training on only 128 paired images per task with frozen text encoders (LoRA: TF), we observe dramatic gains: FID drops from 24.15 to 15.74 for dehazing (35% reduction) and from 37.68 to 12.36 for deraining (67% reduction). For high-noise denoising ( $\sigma = 50$ ), FID improves from 81.75 to 51.98. Interestingly, low-noise denoising ( $\sigma = 15$ ) shows a slight degradation in FID, though CMMD and CLIP-IQA metrics improve substantially. This suggests that while distribution-level statistics may shift, the perceptual quality and feature-space representations become more aligned with ground truth.

**Text encoder fine-tuning.** A critical design choice is whether to keep the text encoders frozen or jointly fine-tune them alongside LoRA adapters. FLUX.1 Kontext employs two pre-trained text encoders (CLIP and T5) that process prompts into conditioning embeddings. Freezing these encoders preserves their general-

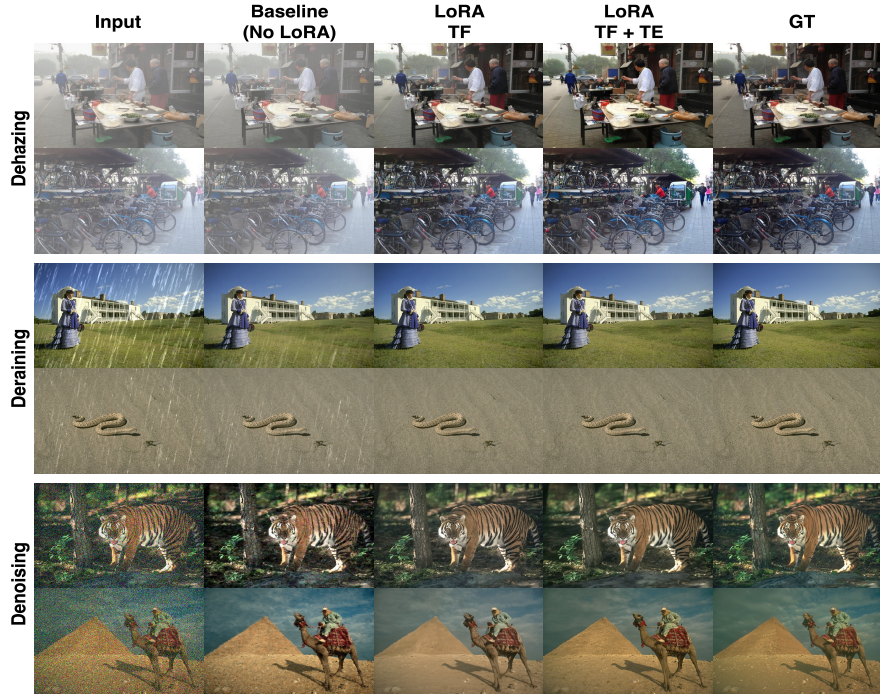


**Fig. 2.** Qualitative comparison of image restoration results.

purpose text understanding, while fine-tuning allows adaptation to restoration-specific semantics—potentially improving alignment between instructions and the corresponding visual transformations. Our results demonstrate consistent advantages from joint fine-tuning (LoRA: TF + TE). For dehazing, both FID and CMMMD improve, indicating better distribution matching with ground truth images. Deraining shows similar trends with FID dropping from 12.36 to 11.76 and CMMMD from 0.42 to 0.40. Across all denoising noise levels, distribution-level metrics improve notably—particularly CMMMD scores, which decrease consistently: at  $\sigma = 15$  from 0.68 to 0.56, at  $\sigma = 25$  from 0.72 to 0.65, and at  $\sigma = 50$  from 0.73 to 0.67. While CLIP-IQA scores remain relatively stable across configurations, the consistent improvements in FID and CMMMD validate that adapting both visual and textual representations enhances the model’s ability to understand and execute restoration instructions.

Figure 2 provides visual evidence of these improvements. The progression from zero-shot to LoRA adaptation, and further to joint text encoder fine-tuning, produces outputs with enhanced structural coherence and more natural appearance. Details are better preserved, artifacts are more effectively removed, and the overall visual fidelity improves substantially. Based on these findings, we adopt joint fine-tuning of text encoders and LoRA adapters for all subsequent

**Table 2.** Data efficiency analysis showing restoration performance across varying training set sizes. All experiments use unified multi-task LoRA ( $r = 64$ ) with text encoder fine-tuning. Metrics are FID/CMMD/CLIP-IQA (lower/lower/higher is better).

Unified Adapter (Per task)	# Pairs	Dehazing		Deraining		Denoising		
		SOTS	Rain100L	$\sigma = 15$	$\sigma = 25$	BSD68 $\sigma = 50$		
✓	128	15.05/0.12/0.59	11.76/0.40/0.91	28.80/0.56/0.89	36.60/0.65/0.88	52.13/0.67/0.88		
	64	15.60/0.14/0.58	11.29/0.41/0.91	28.89/0.58/0.90	35.77/0.63/0.90	51.97/0.73/0.88		
	32	15.20/0.11/0.63	11.92/0.41/0.91	28.64/0.58/0.90	37.12/0.69/0.90	51.99/0.78/0.89		
	16	14.66/0.13/0.60	12.29/0.44/0.91	27.73/0.57/0.90	36.05/0.57/0.89	53.88/0.81/0.88		
✗	16	14.41/0.14/0.60	11.86/0.41/0.90	29.36/0.64/0.89	37.05/0.72/0.88	51.10/0.83/0.88		

experiments, as the consistent distribution-level improvements justify the modest additional computational cost.

### 4.3 Data Efficiency Analysis

A central claim of our work is that pre-trained image editing models can be effectively adapted for restoration with remarkably few training examples. To validate this hypothesis, we systematically investigate the relationship between training set size and restoration quality by varying the number of paired images per task from 16 to 128.

Table 2 presents the results across all restoration tasks using different training set sizes. All experiments use unified multi-task LoRA training with rank  $r = 64$ , text encoder fine-tuning enabled, and are trained for 1,920 iterations to ensure fair comparison. The results demonstrate a striking finding: even with as few as 16 paired images per task (48 total images across three tasks), our method achieves competitive restoration quality across all degradation types.

Examining the metrics across different training set sizes, we observe that performance remains relatively stable as we increase from 16 to 128 pairs. For instance, in dehazing on SOTS, FID scores range from 14.66 to 15.60, while CMMD scores vary from 0.112 to 0.136 across different training sizes. Comparable trends can also be observed for deraining and denoising tasks.

This stability in performance metrics suggests that the pre-trained visual priors in FLUX.1 Kontext are sufficiently rich that even minimal task-specific adaptation (16 pairs) is enough to guide the model toward effective restoration. While we observe some minor fluctuations in metrics as training set size increases, these variations do not follow a consistent monotonic trend, indicating that the model has largely captured the essential restoration patterns from the smallest training set.

### 4.4 Unified Multi-Task vs Task-Specific Adapters

A critical design decision in our parameter-efficient adaptation framework is whether to train separate task-specific LoRA adapters for each restoration operation or employ a single unified adapter that handles multiple degradation types through text prompt conditioning. To investigate this trade-off, we compare two



**Fig. 3.** Qualitative comparison between task-specific and unified multi-task adapters across different restoration tasks. Both configurations produce visually similar results, demonstrating that a single unified adapter can effectively handle multiple degradation types through text prompt conditioning while maintaining quality comparable to specialized task-specific adapters. The unified model offers practical advantages in terms of storage and deployment simplicity without sacrificing restoration quality.

configurations: (1) **Task-specific LoRA**: separate adapters trained independently for each task with 16 paired images, and (2) **Unified LoRA**: a single adapter trained on all three tasks simultaneously (48 total images: 16 per task) with task-specific text prompt conditioning. Both configurations use LoRA rank  $r = 64$  with text encoder fine-tuning enabled.

Table 2 presents the quantitative comparison across all restoration tasks. The results reveal patterns that challenge conventional assumptions about task-specific specialization. For dehazing on SOTS, the unified adapter achieves comparable performance to the task-specific approach across all metrics. For deraining on Rain100L, the task-specific adapter shows slight advantages in FID and CMMMD, while CLIP-IQA scores remain nearly identical, suggesting comparable perceptual quality despite minor differences in distribution-level metrics.

In denoising experiments on BSD68, the unified adapter demonstrates clear advantages at lower noise levels. At  $\sigma = 15$ , it outperforms task-specific training by approximately 1.6 FID points while maintaining identical CLIP-IQA scores. At  $\sigma = 25$ , the unified approach shows superior FID and particularly strong CMMMD improvements. Only at the highest noise level ( $\sigma = 50$ ) does the task-specific adapter gain a modest FID advantage, though perceptual quality metrics remain comparable. These results demonstrate that unified multi-task learning often matches or exceeds task-specific performance in few-shot regimes.

Figure 3 provides visual evidence supporting these findings, showing that unified and task-specific adapters produce comparable visual quality across different degradation types. Beyond performance parity, unified adapters offer substantial practical advantages: a single model handles multiple restoration operations, reducing storage requirements by two-thirds and simplifying deployment. Our findings suggest that unified multi-task learning should be the preferred approach for few-shot restoration, challenging the conventional wisdom that specialized models are necessary for optimal quality.

## 5 Conclusion

We have demonstrated that powerful pre-trained text-conditioned image editing models can be effectively repurposed for image restoration with remarkably few training examples. Our systematic investigation reveals that while FLUX.1 Kontext shows limited restoration capability in zero-shot settings, parameter-efficient LoRA adaptation with only tens of paired images per task unlocks substantial performance improvements across denoising, deraining, and dehazing.

Our comprehensive ablation studies establish three critical insights. First, restoration quality exhibits remarkable stability across varying training set sizes, with even minimal data sufficient to unlock the model’s restoration capabilities. This demonstrates that rich visual priors learned during large-scale editing pre-training can be efficiently transferred to restoration tasks with diminishing returns beyond small training sets. Second, jointly fine-tuning text encoders alongside LoRA adapters consistently improves distribution-level metrics, revealing that adapting both visual and linguistic representations strengthens the alignment between restoration instructions and corresponding image transformations. Third, unified multi-task adapters not only match but often exceed task-specific adapters in few-shot regimes, demonstrating that a single model can effectively handle multiple degradation types through text prompt conditioning while offering significant practical advantages in storage and deployment.

Our work establishes a practical pathway for leveraging large-scale pretrained image editing models in data-scarce restoration scenarios. By demonstrating that sophisticated restoration capabilities can be achieved through parameter-efficient fine-tuning with orders of magnitude fewer examples than traditional training-from-scratch approaches, we open new possibilities for efficient adaptation of generative editing models to inverse problems. Future research could extend this framework to broader restoration tasks, investigate the transferability of editing priors across different architectures, and develop principled methods for determining optimal adaptation strategies based on task characteristics.

**Acknowledgements** This work was supported by Codeway. A.M. Tekalp acknowledges support from Turkish Academy of Sciences (TÜBA).

## References

1. Ai, Y., Huang, H., He, R.: Lora-ir: Taming low-rank experts for efficient all-in-one image restoration. arXiv preprint arXiv:2410.15385 (2024) [3](#)
2. Ai, Y., Huang, H., Zhou, X., Wang, J., He, R.: Multimodal prompt perceiver: Empower adaptiveness, generalizability and fidelity for all-in-one image restoration. arXiv preprint arXiv:2312.02918 (2024) [3](#)
3. Arbeláez, P., Maire, M., Fowlkes, C., Malik, J.: Contour detection and hierarchical image segmentation. IEEE Transactions on Pattern Analysis and Machine Intelligence **33**(5), 898–916 (2011). <https://doi.org/10.1109/TPAMI.2010.161> [7](#)
4. Bilican, A., Yilmaz, M.A., Tekalp, A.M., Cinbiş, R.G.: Exploring sparsity for parameter efficient fine tuning using wavelets. arXiv preprint arXiv:2505.12532 (2025) [4](#)
5. Black Forest Labs, Batifol, S., Blattmann, A., Boesel, F., et al.: FLUX.1 Kontext: Flow matching for in-context image generation and editing in latent space. arXiv preprint arXiv:2506.15742 (2025) [2](#), [4](#)
6. Brooks, T., Holynski, A., Efros, A.A.: Instructpix2pix: Learning to follow image editing instructions. arXiv preprint arXiv:2211.09800 (2022) [4](#)
7. Cai, Y., Bian, H., Lin, J., Wang, H., Timofte, R., Zhang, Y.: Retinexformer: One-stage retinex-based transformer for low-light image enhancement. In: Proceedings of the IEEE/CVF International Conference on Computer Vision (ICCV). pp. 12504–12513 (October 2023) [3](#)
8. Chen, L., Chu, X., Zhang, X., Sun, J.: Simple baselines for image restoration. arXiv preprint arXiv:2204.04676 (2022) [3](#)
9. Chen, L., Lu, X., Zhang, J., Chu, X., Chen, C.: Hinet: Half instance normalization network for image restoration. In: Proceedings of the IEEE/CVF Conference on Computer Vision and Pattern Recognition (CVPR) Workshops. pp. 182–192 (June 2021) [3](#)
10. Chen, S., Ye, T., Liu, Y., Chen, E., Shi, J., Zhou, J.: Snowformer: Scale-aware transformer via context interaction for single image desnowing. arXiv preprint arXiv:2208.09703 (2022) [3](#)
11. Chen, X., Wu, Z., Liu, X., Pan, Z., Liu, W., Xie, Z., Yu, X., Ruan, C.: Janus-pro: Unified multimodal understanding and generation with data and model scaling. arXiv preprint arXiv:2501.17811 (2025) [4](#)
12. Conde, M.V., Geigle, G., Timofte, R.: InstructIR: High-quality image restoration following human instructions. In: Eur. Conf. Comput. Vis. (2024) [2](#), [3](#)
13. Fan, Q., Chen, D., Yuan, L., Hua, G., Yu, N., Chen, B.: A general decoupled learning framework for parameterized image operators. IEEE Transactions on Pattern Analysis and Machine Intelligence **43**(1), 33–47 (2021). <https://doi.org/10.1109/TPAMI.2019.2925793> [7](#)
14. Heusel, M., Ramsauer, H., Unterthiner, T., Nessler, B., Hochreiter, S.: Gans trained by a two time-scale update rule converge to a local nash equilibrium. In: Guyon, I., Luxburg, U.V., Bengio, S., Wallach, H., Fergus, R., Vishwanathan, S., Garnett, R. (eds.) Advances in Neural Information Processing Systems. vol. 30. Curran Associates, Inc. (2017), [https://proceedings.neurips.cc/paper\\_files/paper/2017/file/8a1d694707eb0fefe65871369074926d-Paper.pdf](https://proceedings.neurips.cc/paper_files/paper/2017/file/8a1d694707eb0fefe65871369074926d-Paper.pdf) [7](#)
15. Hu, E.J., Shen, Y., Wallis, P., Allen-Zhu, Z., Li, Y., Wang, S., Wang, L., Chen, W.: LoRA: Low-rank adaptation of large language models. In: Int. Conf. Learn. Represent. (2022) [2](#), [4](#)

16. Jayasumana, S., Ramalingam, S., Veit, A., Glasner, D., Chakrabarti, A., Kumar, S.: Rethinking fid: Towards a better evaluation metric for image generation. In: 2024 IEEE/CVF Conference on Computer Vision and Pattern Recognition (CVPR). pp. 9307–9315 (2024). <https://doi.org/10.1109/CVPR52733.2024.00889> 7
17. Jiang, K., Wang, Z., Yi, P., Chen, C., Huang, B., Luo, Y., Ma, J., Jiang, J.: Multi-scale progressive fusion network for single image deraining. In: IEEE/CVF Conference on Computer Vision and Pattern Recognition (CVPR) (June 2020) 3
18. Jiang, Y., Zhang, Z., Xue, T., Gu, J.: Autodir: Automatic all-in-one image restoration with latent diffusion. arXiv preprint arXiv:2310.10123 (2023) 3
19. Kupyn, O., Budzan, V., Mykhailych, M., Mishkin, D., Matas, J.: Deblurgan: Blind motion deblurring using conditional adversarial networks. ArXiv e-prints (2017) 3
20. Li, B., Ren, W., Fu, D., Tao, D., Feng, D., Zeng, W., Wang, Z.: Benchmarking single-image dehazing and beyond. IEEE Transactions on Image Processing **28**(1), 492–505 (2019). <https://doi.org/10.1109/TIP.2018.2867951> 7
21. Li, B., Liu, X., Hu, P., Wu, Z., Lv, J., Peng, X.: All-in-one image restoration for unknown corruption. In: IEEE Conf. Comput. Vis. Pattern Recog. pp. 17452–17462 (2022) 2, 3
22. Li, Z., Lei, Y., Ma, C., Zhang, J., Shan, H.: Prompt-in-prompt learning for universal image restoration. arXiv preprint arXiv:2312.05038 (2023) 3
23. Liang, J., Cao, J., Sun, G., Zhang, K., Van Gool, L., Timofte, R.: SwinIR: Image restoration using swin transformer. In: IEEE Int. Conf. Comput. Vis. Workshops. pp. 1833–1844 (2021) 3
24. Lin, X., He, J., Chen, Z., Lyu, Z., Dai, B., Yu, F., Ouyang, W., Qiao, Y., Dong, C.: Diffbir: Towards blind image restoration with generative diffusion prior. arXiv preprint arXiv:2308.15070 (2024) 3
25. Lipman, Y., Chen, R.T.Q., Ben-Hamu, H., Nickel, M., Le, M.: Flow matching for generative modeling. In: Int. Conf. Learn. Represent. (2023) 5
26. Liu, X., Gong, C., Liu, Q.: Flow straight and fast: Learning to generate and transfer data with rectified flow. In: Int. Conf. Learn. Represent. (2023) 5
27. Liu, Y.F., Jaw, D.W., Huang, S.C., Hwang, J.N.: Desnownet: Context-aware deep network for snow removal. IEEE Transactions on Image Processing **27**(6), 3064–3073 (2018) 3
28. Loshchilov, I., Hutter, F.: Decoupled weight decay regularization. In: International Conference on Learning Representations (2019), <https://openreview.net/forum?id=Bkg6RiCqY7> 7
29. Luo, Z., Gustafsson, F.K., Zhao, Z., Sjölund, J., Schön, T.B.: Controlling vision-language models for universal image restoration. arXiv preprint arXiv:2310.01018 (2023) 3
30. Ma, J., Cheng, T., Wang, G., Wang, X., Zhang, Q., Zhang, L.: Prores: Exploring degradation-aware visual prompt for universal image restoration. arXiv preprint arXiv:2306.13653 (2023) 3
31. Ma, Y., Liu, X., Chen, X., Liu, W., Wu, C., Wu, Z., Pan, Z., Xie, Z., Zhang, H., yu, X., Zhao, L., Wang, Y., Liu, J., Ruan, C.: Janusflow: Harmonizing autoregression and rectified flow for unified multimodal understanding and generation. arXiv preprint arXiv:2411.07975 (2024) 4
32. Nah, S., Kim, T.H., Lee, K.M.: Deep multi-scale convolutional neural network for dynamic scene deblurring. In: The IEEE Conference on Computer Vision and Pattern Recognition (CVPR) (July 2017) 3
33. Potlapalli, V., Zamir, S.W., Khan, S., Khan, F.S.: PromptIR: Prompting for all-in-one blind image restoration. In: Adv. Neural Inform. Process. Syst. (2023) 2, 3

34. Qian, R., Tan, R.T., Yang, W., Su, J., Liu, J.: Attentive generative adversarial network for raindrop removal from a single image. In: The IEEE Conference on Computer Vision and Pattern Recognition (CVPR) (June 2018) 3
35. Qin, X., Wang, Z., Bai, Y., Xie, X., Jia, H.: Ffa-net: Feature fusion attention network for single image dehazing. In: Proceedings of the AAAI Conference on Artificial Intelligence. vol. 34, pp. 11908–11915 (2020) 3
36. Radford, A., Kim, J.W., Hallacy, C., Ramesh, A., Goh, G., Agarwal, S., Sastry, G., Askell, A., Mishkin, P., Clark, J., et al.: Learning transferable visual models from natural language supervision. In: International Conference on Machine Learning (ICML). pp. 8748–8763 (2021) 5
37. Raffel, C., Shazeer, N., Roberts, A., Lee, K., Narang, S., Matena, M., Zhou, Y., Li, W., Liu, P.J.: Exploring the limits of transfer learning with a unified text-to-text transformer. *Journal of Machine Learning Research* **21**(140), 1–67 (2020) 5
38. Tian, Y., Han, J., Chen, H., Xi, Y., Ding, N., Hu, J., Xu, C., Wang, Y.: Instruct-ipt: All-in-one image processing transformer via weight modulation. *arXiv preprint arXiv:2407.00676* (2024) 3
39. Wang, J., Chan, K.C., Loy, C.C.: Exploring clip for assessing the look and feel of images. In: AAAI (2023) 7
40. Wang, J., Yue, Z., Zhou, S., Chan, K.C.K., Loy, C.C.: Exploiting diffusion prior for real-world image super-resolution. *arXiv preprint arXiv:2305.07015* (2024) 3
41. Wang, Z., Cun, X., Bao, J., Zhou, W., Liu, J., Li, H.: Uformer: A general u-shaped transformer for image restoration. In: Proceedings of the IEEE/CVF Conference on Computer Vision and Pattern Recognition (CVPR). pp. 17683–17693 (June 2022) 3
42. Wei, C., Wang, W., Yang, W., Liu, J.: Deep retinex decomposition for low-light enhancement. In: British Machine Vision Conference. British Machine Vision Association (2018) 3
43. Wu, C., Li, J., Zhou, J., Lin, J., Gao, K., Yan, K., ming Yin, S., Bai, S., Xu, X., Chen, Y., Chen, Y., Tang, Z., Zhang, Z., Wang, Z., Yang, A., Yu, B., Cheng, C., Liu, D., Li, D., Zhang, H., Meng, H., Wei, H., Ni, J., Chen, K., Cao, K., Peng, L., Qu, L., Wu, M., Wang, P., Yu, S., Wen, T., Feng, W., Xu, X., Wang, Y., Zhang, Y., Zhu, Y., Wu, Y., Cai, Y., Liu, Z.: Qwen-image technical report. *arXiv preprint arXiv:2508.02324* (2025) 4
44. Xiao, S., Wang, Y., Zhou, J., Yuan, H., Xing, X., Yan, R., Wang, S., Huang, T., Liu, Z.: Omnigen: Unified image generation. *arXiv preprint arXiv:2409.11340* (2024) 4
45. Zamir, S.W., Arora, A., Khan, S., Hayat, M., Khan, F.S., Yang, M.H.: Restormer: Efficient transformer for high-resolution image restoration. In: IEEE Conf. Comput. Vis. Pattern Recog. pp. 5728–5739 (2022) 3
46. Zamir, S.W., Arora, A., Khan, S., Hayat, M., Khan, F.S., Yang, M.H., Shao, L.: Multi-stage progressive image restoration. In: CVPR (2021) 3
47. Zhang, K., Zuo, W., Chen, Y., Meng, D., Zhang, L.: Beyond a gaussian denoiser: Residual learning of deep cnn for image denoising. *IEEE Transactions on Image Processing* **26**(7), 3142–3155 (2017). <https://doi.org/10.1109/TIP.2017.2662206> 3
48. Zhang, Y., Zhang, H., Chai, X., Cheng, Z., Xie, R., Song, L., Zhang, W.: Diff-restorer: Unleashing visual prompts for diffusion-based universal image restoration. *arXiv preprint arXiv:2407.03636* (2024) 3
49. Zhou, K., Yang, J., Loy, C.C., Liu, Z.: Learning to prompt for vision-language models. *International Journal of Computer Vision (IJCV)* (2022) 4